Supplementary Figure S1 (Related to Figure 1)

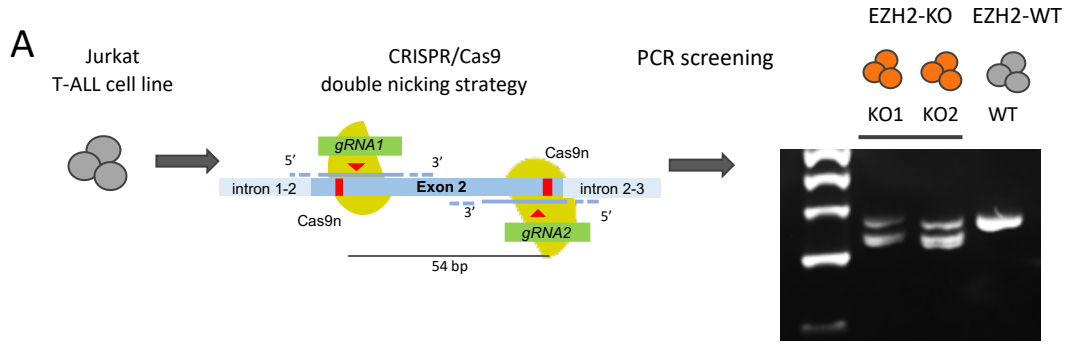

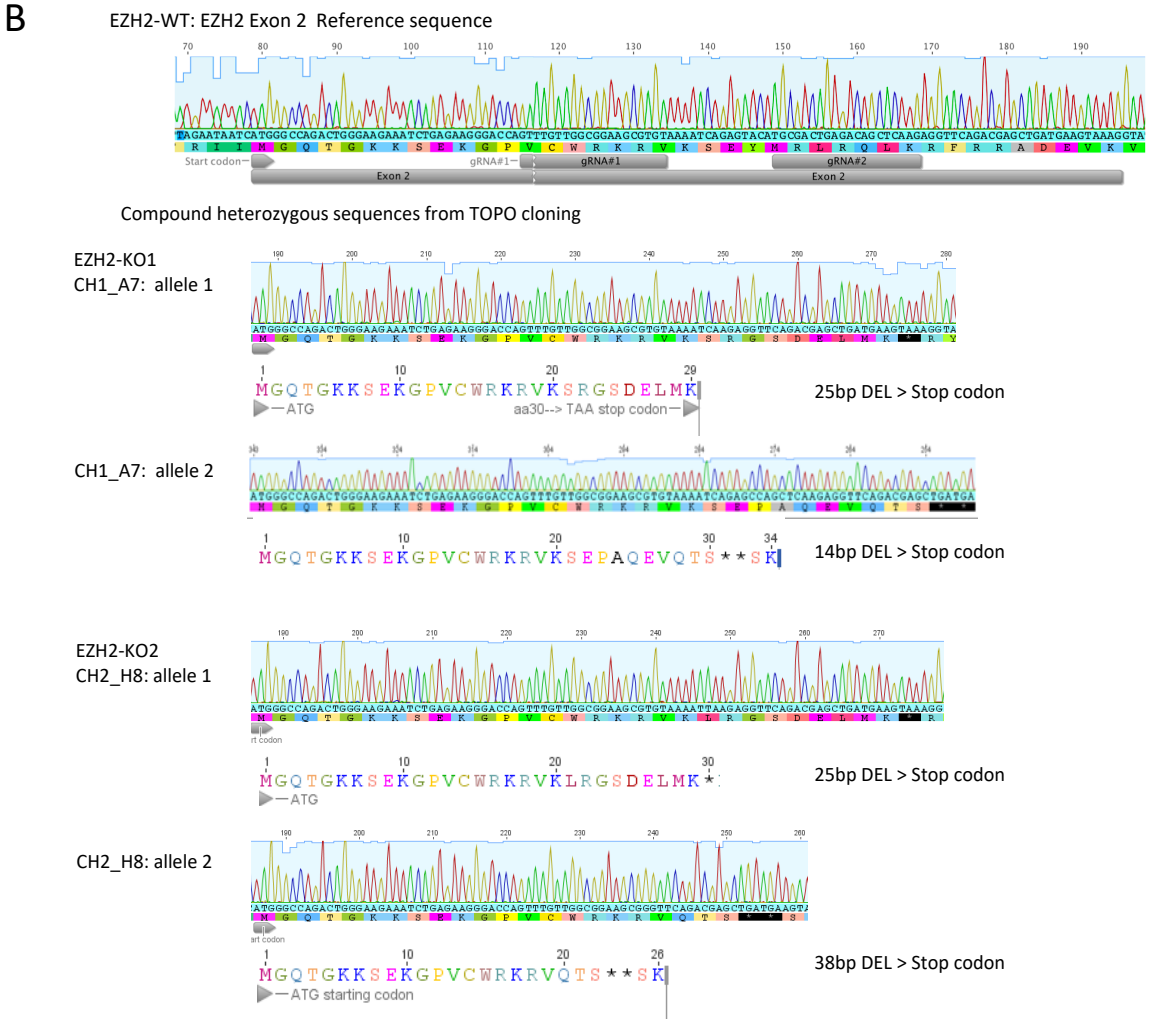

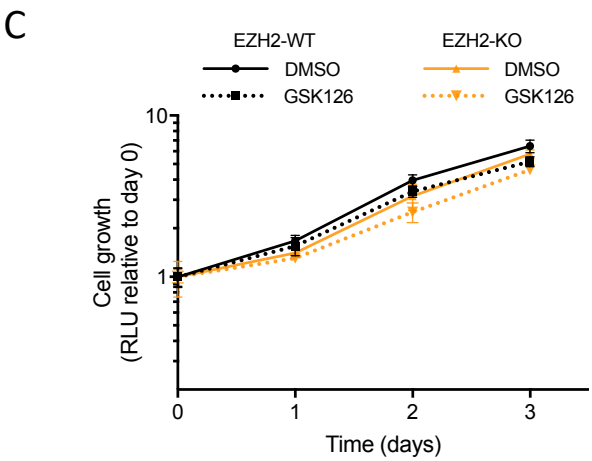

Supplementary Figure S1 (related to Fig. 1)

A) Double Nickase strategy used for generation of Jurkat EZH2-KO cell lines, and PCR products of the CRISPR/Cas9-deleted region in exon 2 *EZH2* analysed by agarose gels, showing the mutated alleles in EZH2-KO1 and EZH2-KO2 clones. The upper band observed in the EZH2-KO clones represents a heteroduplex of the two mutant alleles. B) Sequencing traces of each CRISPRed allele of EZH2-KO1 and EZH2-KO2 cells, obtained from TOPO- cloning of exon 2 *EZH2* PCR products. Translation of the sequences obtained using Geneious software showing generation of stop codons, are indicated in the figure (*). EZH2-WT sequence showing the gRNA sites are included as a reference. C) Growth curve of Jurkat EZH2-WT and EZH2-KO cell lines incubated with GSK126. Cells were pre-incubated with GSK126 (2μM) or DMSO (control) for 7 days, after which point, they were plated in 96 well plates in complete medium with and without GSK126. Cell growth was determined at each time point using CellTiter Glo.

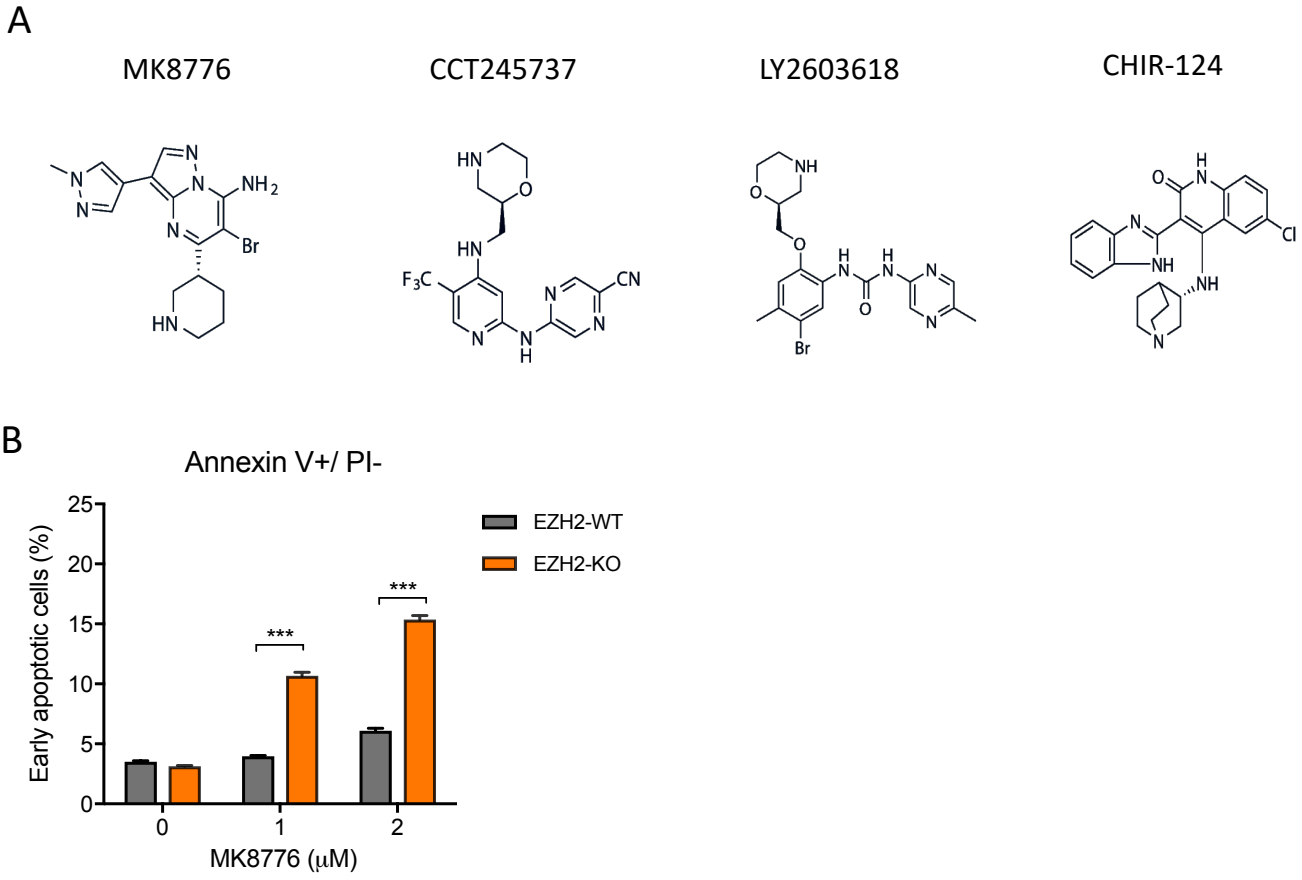

Supplementary Figure S2 (related to Fig. 1)

A) Chemical structure of four different CHK1 inhibitors tested in this study. B) Percentage of early apoptotic (Annexin V+/PI-) cells following 24 hours of treatment. EZH2-WT and -KO cells incubated at increasing doses of MK8776, were collected for FACS analysis using FITC Annexin V and propidium iodide (PI) solutions. Bars represent the mean of one experiment performed in triplicates. Significance was assessed by Student's t-test, *** *P* value <0.001

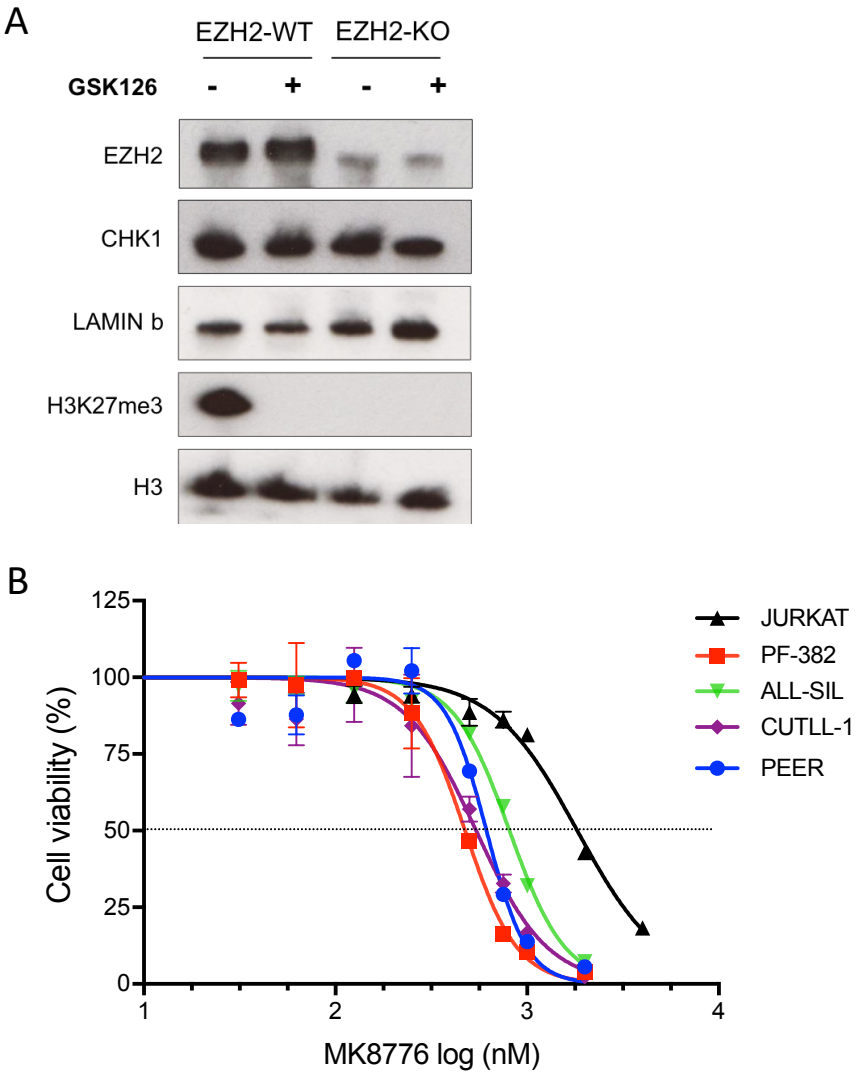

Supplementary Figure S3 (related to Fig. 2)

A) Western blot (WB) of cell lysates from Jurkat EZH2-WT and EZH2-KO cells, pre- incubated with 2μM GSK126 or DMSO (control) for 7 days. The WB shows downregulation of global H3K27me3 in EZH2-WT, and no changes in total CHK1 or EZH2 expression in both cell lines, following GSK126 treatment. LAMIN b is shown as loading control. B) Dose response to CHK1 inhibitor MK8776 in T-ALL cell lines. Cells were incubated with increasing doses of the compound for 72 hr. Cell viability was determined using CellTiter Glo.

Supplementary Figure S4 (Related to Figure 3)

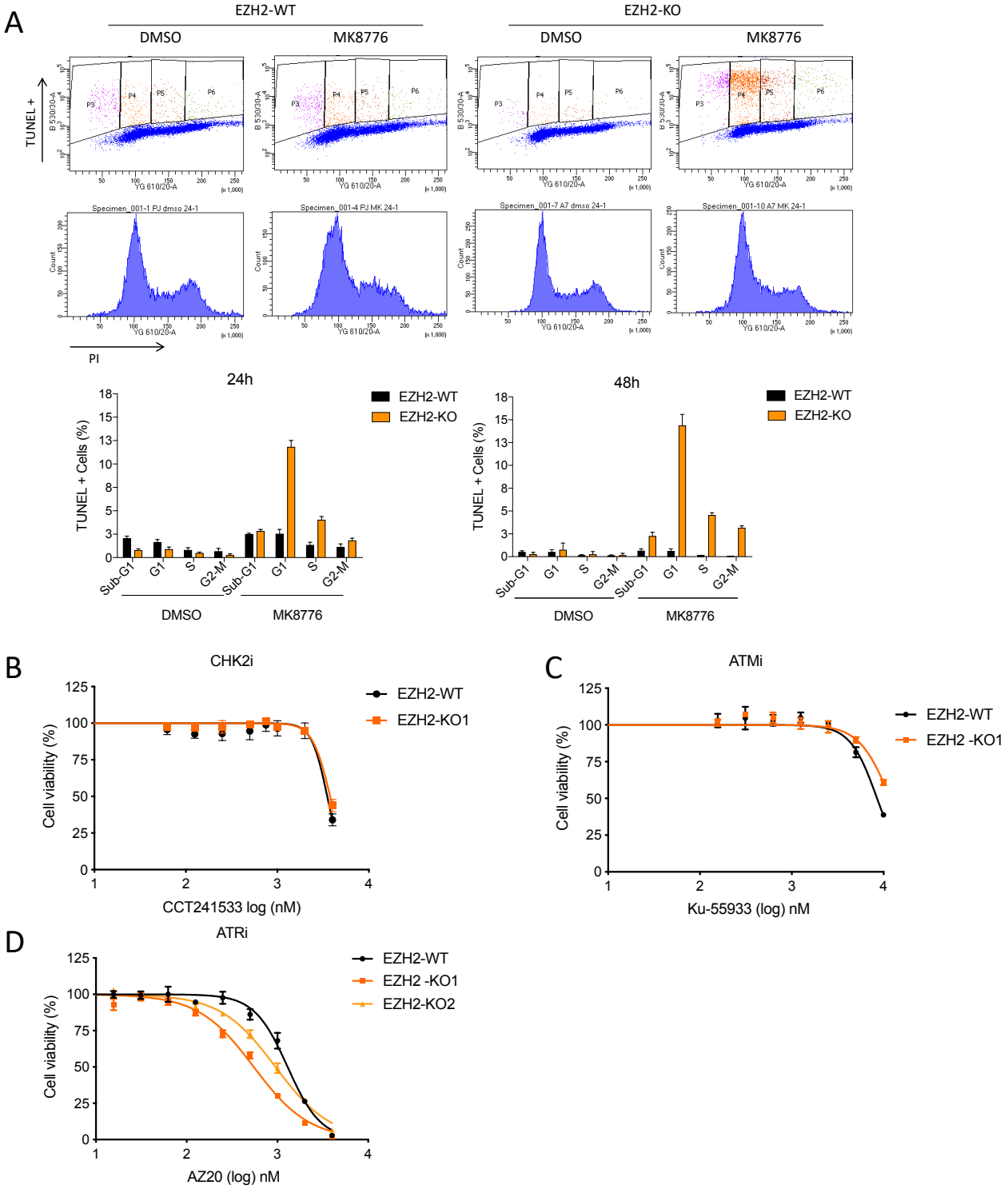

Supplementary Figure S4 (related to Fig. 3)

A) APO-BrdU TUNEL assay performed in EZH2-WT and EZH2-KO Jurkat cells, incubated with CHK1 inhibitor MK8776. Upper panel shows TUNEL + vs. PI staining flow cytometry plots from one replicate (24 hours treatment) of experiment performed in triplicates. Lower panel shows percentages of TUNEL positive cells obtained upon 24 and 48 hours MK8776 treatment, bars represent mean of triplicates. B-D) Dose response to CHK2 inhibitor (CHK2i) CCT241533, (C) ATM inhibitor (ATMi) Ku- 55933, and (D) ATR inhibitor (ATRi) AZ20 in EZH2-WT versus EZH2-KO cells. Cells were incubated with increasing doses of each compound for 72 hours, and cell viability was determined using CellTiter Glo.

Supplementary Figure S5 (Related to Figure 4)

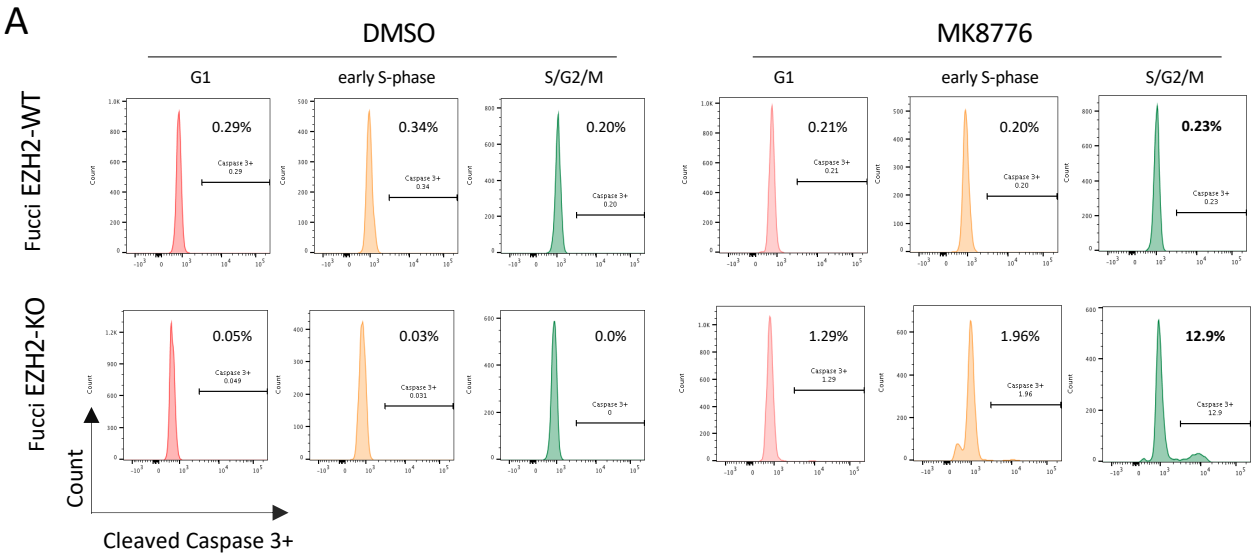

Supplementary Figure S5 (related to Fig. 5)

A) Cleaved-Caspase-3 flow cytometric analysis of FucciEZH2-WT and FucciEZH2-KO Jurkat cells, following DMSO or MK8776 (2μM) treatment for 24 hours, in relation to their cell cycle stage. One representative image of experiment performed in triplicates. An increased percentage of cleaved-Caspase 3 positive cells is observed in MK8776 treated FucciEZH2-KO population, particularly in S/G2/M stages of the cell cycle.

Supplementary Figure S6 (Related to Figure 5)

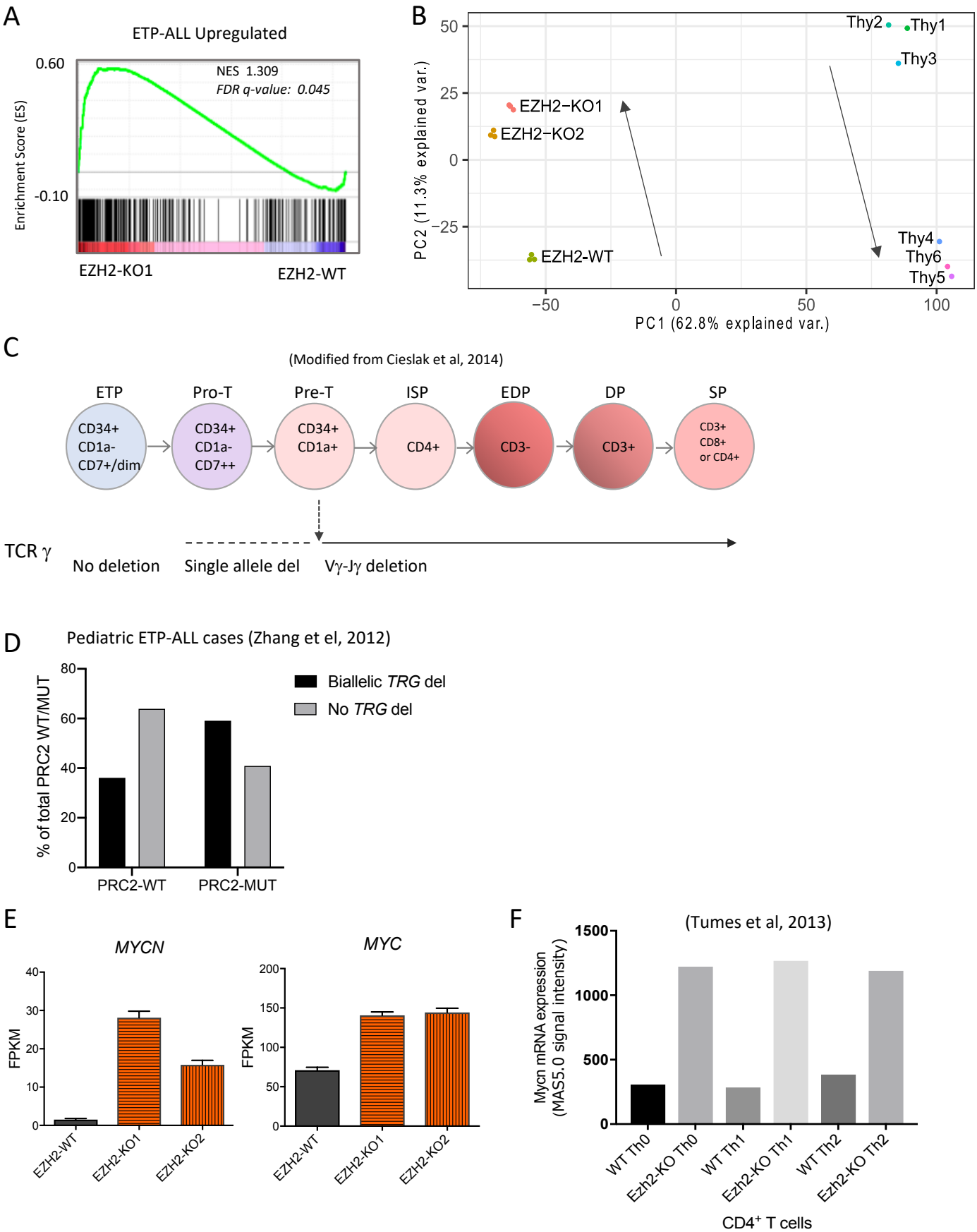

Supplementary Figure S6 (related to Fig. 5)

A) GSEA analysis of EZH2-KO1 and EZH2-WT cells for genes upregulated in human ETP- ALL relative to non-ETP T-ALL cases (Zhang et al, 2012). NES, normalized enrichment score; FDR *q*-value, false discovery rate *q* value. B) Principal component analysis of RNA-seq data from EZH2-WT and EZH2-KO Jurkat cells (*n*=3 biological replicates), including thymic subsets from Casero et al., 2015 (compiled data from *n*=2 biological replicates per population). PC1 separates Jurkat cell lines from thymic primary cells, while PC2 captures the differentiation status of the primary cells and shows how EZH2-KO mimic a reversion to an earlier phenotype. C) Thymic maturation stages and their TCRg rearrangements in humans, modified from Cieslak et al, 2014. D) Frequency of biallelic *TRG* deletion and no deletion (absence of biallelic deletion), with and without mutations in PRC2 genes, in the ETP-ALL subgroup of pediatric T-ALL cases from Zhang et al., 2012. Given contamination with normal cell DNA can lead to apparent hemizygosity, these patients were excluded from the analysis (n=6). E) Quantification of fragments per kilobase million (FPKM) of *MYCN* and *MYC* from RNA-seq analysis of EZH2-WT and EZH2-KO Jurkat cells. Bar graphs represent the mean ± SD of triplicates. F) *Mycn* mRNA relative expression in Ezh2-WT or Ezh2-KO -CD4+ T cell populations, as reported in Tumes et al, 2013.

Supplementary Figure S7 (Related to Figure 6)

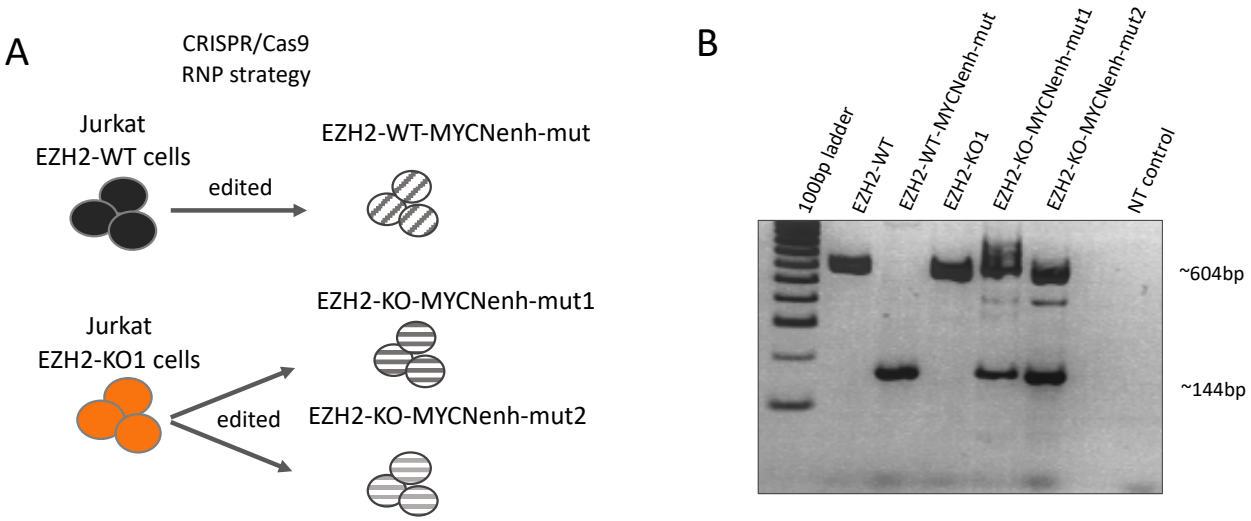

Supplementary Figure S7 (related to Fig. 6)

A) Schematic diagram of the CRISPR/Cas9 RNP strategy used to edit the MYCN enhancer in EZH2-WT and EZH2-KO1 Jurkat cells. B) Agarose gel of PCR products obtained during the CRISPR screening, showing a deletion of ~460bp in EZH2-WT-MYCNenh-mut and EZH2- KO-MYCNenh-mut1 and EZH2-KO-MYCNenh-mut2. Sanger sequencing of PCR products from EZH2-KO-MYCNenh-mut2 showed the upper band (~604bp) contained an inversion of the WT sequence, confirming compound heterozygous mutations in these clones.

Supplementary Figure S8 (Related to Figure 7)

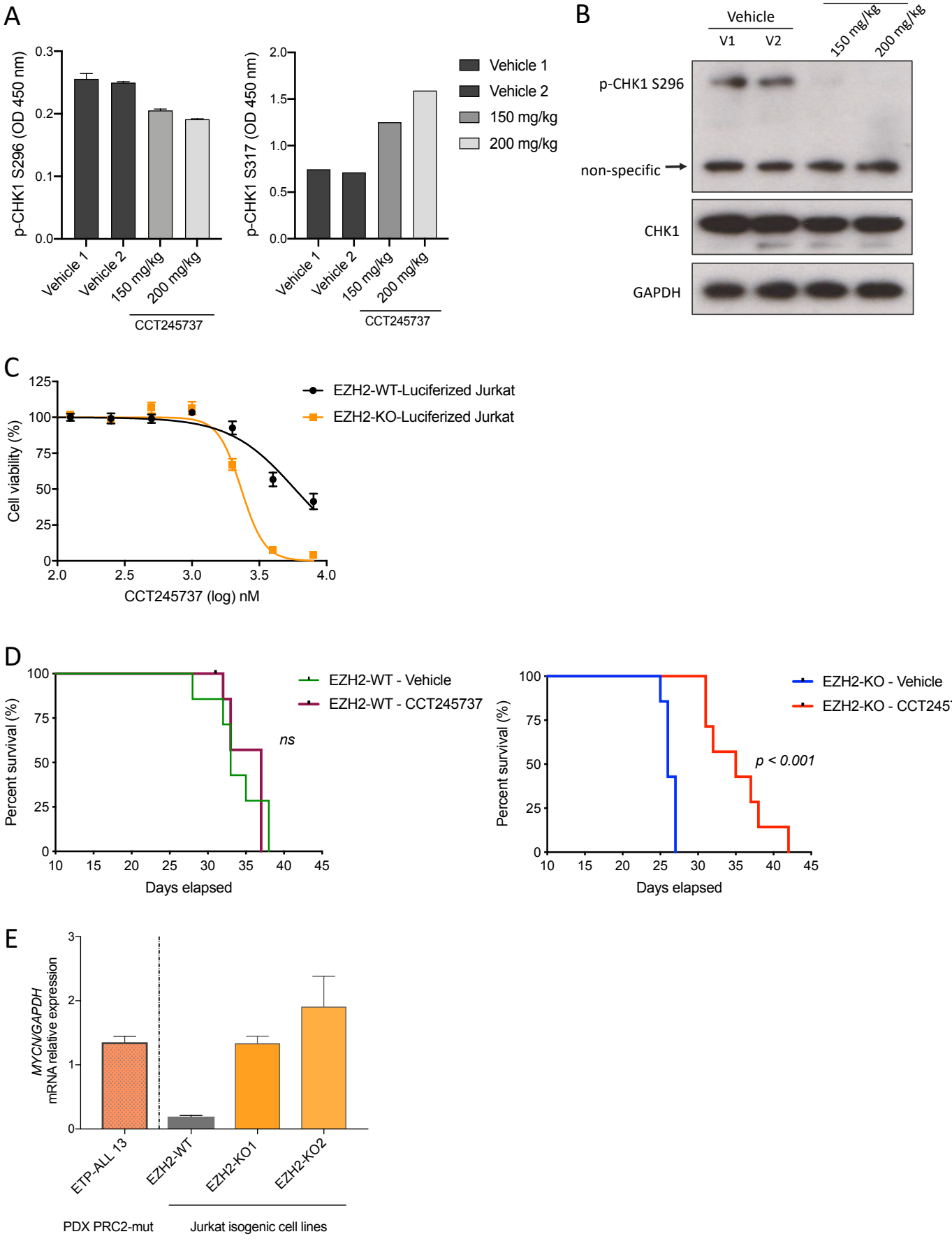

Supplementary Figure S8 (related to Fig. 7)

A) ELISA assays for phospho-CHK1 S296 (CHK1 autophosphorylation activity) and phospho-CHK1 S317 (ATR mediated phosphorylation, as a marker of replication stress response activation) were performed from PDX ETP-ALL13 tumor homogenates. Spleen tissue was harvested 4 hours following CCT245737 or Vehicle P.O. at indicated doses, and ELISA assay was performed as indicated in the methods section. B) Western blotting confirmation of phospho-CHK1 S296 levels in tumor homogenates obtained in (A) was performed using the same antibody. Total CHK1 and GAPDH expression levels are shown as loading controls. C) Dose-response to CHK1 inhibitor CCT245737 in EZH2-WT and EZH2-KO-luciferized Jurkat cells. Luciferase expressing Jurkat cells, obtained from bone marrow of engrafted NSG mice, were allowed to grow in puromycin containing medium. Cells were then incubated at increasing doses of CCT245737 for 72 hr, and cell viability was determined using CellTiter Glo. Results show mean ± SD of two experiments performed in triplicate. D) Kaplan–Meier survival curves comparing mice injected with EZH2-WT-luciferized Jurkat cells (left panel) and mice injected with EZH2-KO-luciferized Jurkat cells (right panel). CCT245737 (150mg/kg P.O.) was administered on D10-15, 17-21, 24-28, 31-35, post IV injection of tumor cells, $n = 7$ mice per group ($P = 0.0003$, by log-rank Mantel-Cox test)). E) mRNA MYCN expression levels in ETP-ALL patient derived xenograft (PDX) ETP-ALL-13, compared with Jurkat EZH2-WT and EZH2-KO cells, as determined by Q-PCR analysis.